applied sciences

MDPI

Article

Topology Optimization Design and Experimental Research of a 3D-Printed Metal Aerospace Bracket Considering Fatigue Performance

Yisheng Chen [1,2], Qianglong Wang [1,2], Chong Wang [1], Peng Gong [1], Yincheng Shi [1,2], Yi Yu [1,2] and Zhenyu Liu [1,2,*]

[1] Changchun Institute of Optics, Fine Mechanics and Physics (CIOMP), Chinese Academy of Sciences, Changchun 130033, China; chenyisheng17@mails.ucas.ac.cn (Y.C.); lqwang14@foxmail.com (Q.W.); wangchong@ciomp.ac.cn (C.W.); gongpeng0010@163.com (P.G.); yinchengshi@foxmail.com (Y.S.); 13756006195@139.com (Y.Y.)

[2] School of Optoelectronics, University of Chinese Academy of Sciences, Beijing 100049, China

* Correspondence: liuzy@ciomp.ac.cn

Abstract: In the aerospace industry, spacecraft often serve in harsh operating environments, so the design of ultra-lightweight and high-performance structures is a major requirement in aerospace structure design. In this article, a lightweight aerospace bracket considering fatigue performance was designed by topology optimization and manufactured by 3D-printing. Considering the requirements of assembly with a fixture for fatigue testing and avoiding stress concentration, a reconstructed model was presented by CAD software before manufacturing. To improve the fatigue performance of the structure, this article proposes the design idea of abstracting the practiced working condition of the bracket subjected to cycle loads in the vertical direction via a multiple load-case topology optimization problem by minimizing compliance under a variety of asymmetric extreme loading conditions. Parameter sweeping was used to improve the computational efficiency. The mass of the new bracket was reduced by 37% compared to the original structure. Both numerical simulation and the fatigue test were implemented to support the validity of the new bracket. This work indicates that the integration of the proposed topology optimization design method and additive manufacturing can be a powerful tool for the design of lightweight structures considering fatigue performance.

Keywords: topology optimization; additive manufacturing; fatigue testing; COMSOL

Citation: Chen, Y.; Wang, Q.; Wang, C.; Gong, P.; Shi, Y.; Yu, Y.; Liu, Z. Topology Optimization Design and Experimental Research of a 3D-Printed Metal Aerospace Bracket Considering Fatigue Performance. *Appl. Sci.* **2021**, *11*, 6671. https://doi.org/10.3390/app11156671

Academic Editor: Julio Marti

Received: 24 June 2021
Accepted: 12 July 2021
Published: 21 July 2021

1. Introduction

Additive manufacturing technology such as 3D-printing provides a new way of manufacturing complex components by printing structures layer by layer with materials [1]. Topology optimization is a structural optimization design method to distribute materials reasonably and to determine the optimal force transmitting path according to the specified load conditions, performance indicators, and constraints [2]. On comparison with size optimization and shape optimization, topology optimization does not depend on the choice of the initial configuration and offers a wider design space. Therefore, it is an effective design method for seeking high performance, lightweight, and multiple innovative structures, and has been applied extensively in aerospace [3,4] heat transfer systems [5], and architectural design [6]. For example, the European Aeronautic Defence and Space company (EADS) Innovation Works optimized the Airbus A320 cabin hinge bracket by topology optimization and manufactured the topology optimization results using additive manufacturing. The new structure has a 60% weight reduction compared to the original structure design while meeting the strength requirements [7]. Thales Alenia Space (France) and Poly-shape (a 3D printing service company), designed and printed the antenna mount structure for the new Korean communication satellites Koreasat-5A and Koreasat-7 with 22% weight reduction compared to the conventional structure [8]. The combination of

topology optimization and additive manufacturing provides a reliable path to compactness, integrated layout, and lightweight structure design [9].

The continuum topology optimization method has been fruitfully undergoing development over the last several decades [2,10–12]. After many years of research and development, there are three major approaches in the field of topology optimization, which are the Solid Isotropic Material with Penalization (SIMP) method, the Evolutionary Structural Optimization (ESO)/Bidirectional Evolutionary Structural Optimization (BESO) method, and the level set method. Respectively, each of these methods has its own characteristics: the SIMP method is simple and convenient to implement numerically; the ESO/BESO method optimizes the results without intermediate density region; the level set method can clearly describe the boundary of the optimization results. In this article, the SIMP method is used because it is convenient to implement.

Under periodic cyclic loading, most components are vulnerable to fatigue failure, which makes the service life of the components much shorter. There has been some work on fatigue-resistant design using topology optimization methods. Jie, et al. [13] proposed the simulation of the stress state at the joint using a combined element and introduced the fatigue criterion as a constraint to the topology optimization design, while the p-norm equation was also used to improve the computational efficiency, which was aimed at fatigue performance of multi riveted joint structures. However, the author did not elaborate further on the accuracy of simulated stresses using combined elements. Shanglong, et al. [14] investigated the topology optimization problem considering fatigue properties under asymmetric loading and described the complete time course of asymmetric loading action as a linear superposition of a series of unit static loads to ease the computationally burdensome problem of topology optimization under asymmetric loading. In paper [14], there is a 3D industrial example with a large grayscale result, which indicates that there is still potential to improve the convergence of the algorithm. Desmorat and Desmorat [15] studied the topology optimization of structures at low periodic cycle, where the fatigue of the material was strongly influenced by the plasticity of the material, and by introducing the Lemaitre material damage criterion, the fatigue life of the structure was optimized to the greatest extent. Collet, et al. [16] investigated the topology optimization problem considering fatigue resistance properties by introducing a modified Goodman criterion and Sines equivalent mean stresses and showed that the optimized structure was able to avoid some stress concentrations due to geometric singularities. However, the paper only shows the results of two-dimensional examples and does not extend the algorithm to three-dimensional examples. Therefore, it remains to be seen whether the algorithm can be applied to practical engineering 3D structures. Holmberg, et al. [17] converted the fatigue constraints of the structure to stress constraints based on the Palmgren–Miner linear cumulative damage criterion, as well as using the strategy of separating fatigue analysis from topology optimization to design the structure with the goal of minimum mass to ensure that the structure did not fail during operation. Although the overall stress level was reduced in the optimization results, the reduction of the stress value at the geometric singularities was not obvious. Nabaki, et al. [18] applied the BESO method to study the topology optimization fatigue problem under a high cycle for research, which improved the computational efficiency of the algorithm by introducing a modified Goodman criterion and a modified equation; numerical examples were presented to prove the effectiveness of the algorithm. There are various criterion mentioned in paper [17,18], the basic idea of which is to control the stress amplitude of the structure within the range allowed by the criterion in the process of structural design. This paper utilizes a similar design idea which ensures that the von-Mises stress values of the redesigned bracket are within a reasonable range. A fatigue test is also performed on the redesigned bracket after 3D-printing and the test result shows that the redesigned bracket can satisfy the expected engineering specifications.

This article mainly considers the application of topology-optimized structural design for fatigue characteristics. The article is presented as follows. In Section 2, the detailed

design requirements of the aerospace bracket are presented. Section 3 introduces the design model of the aerospace bracket considering fatigue characteristics. The topology optimization model considering fatigue characteristics and its sensitivity analysis are presented. In Section 4, the result of the proposed method is given, in addition to the geometry model reconstructed by reverse engineering. Meanwhile, the simulation results of the new geometry and the original geometry under the same load are compared. In Section 5, the experimental procedure and the experimental result of the new bracket fabricated using 3D-printing are shown. In Section 6, the article is summarized.

2. The Design Requirement of the Aerospace Bracket

The original aerospace bracket is a connecting piece in aerospace equipment, the structure of which is shown in Figure 1. The schematic diagram of the assembly of the original bracket and the fatigue testing platform are shown in Figure 2. From Figure 2 where it can be seen that the vertical plate and the bottom plate of the original bracket structure have a number of through-holes, which are all connected to the fixture with bolts, as well as being subjected to a sine load in the vertical direction together with other components. In response to the design requirement of a lightweight aerospace bracket, the material of the bracket is high-strength alloy TC4. The chemical composition of TC4 alloy is shown in Table 1. The new bracket should satisfy engineering specification while being as light as possible. This demands that the designed bracket is required to meet the requirement of more than 10,000 cycles without failure under a maximum load of 50 kN and a minimum load of 5 kN vertical cycle load on a fatigue test machine. Prior to new bracket design, static analysis is conducted with the commercial finite element software COMSOL to determine its mechanical properties. In finite element analysis, it is assumed that all the bolts of the bracket are well fixed during the loading process, which means that the restraint should be set to be fixed near the bolt holes of the bottom and the lower part of the three bolt holes above the vertical plate which is subjected to a total vertical direction load of 50 kN. The restraint boundary and load condition are shown in Figure 3. The lower part of the three bolt holes above the vertical plate is subjected to a total vertical downward load of 50 kN and the numerical simulation of the result is shown in Figure 4.

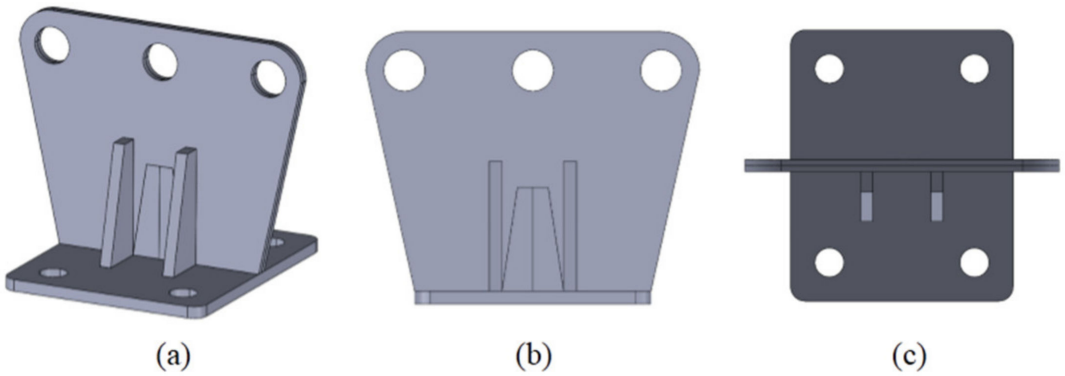

Figure 1. Original structure of the aerospace bracket. (**a**) represents the angle-specific view of original structure; (**b**) represents front view of original structure; (**c**) represents top view of original structure.

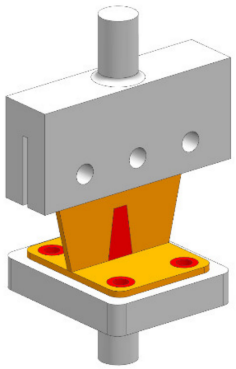

Figure 2. The schematic diagram of the assembly of the original bracket and the fatigue testing platform.

Table 1. Chemical composition of TC4 alloy (weight%).

Elements			Impurity Elements, Max						
Al	V	Ti	Fe	C	N	H	O	Other Elements	
								Each	All
5.5 ~ 6.75	3.5 ~ 4.5	The rest	0.3	0.08	0.05	0.015	0.2	0.1	0.4

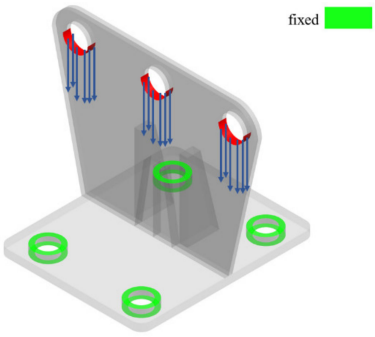

Figure 3. Boundary condition and load condition setting.

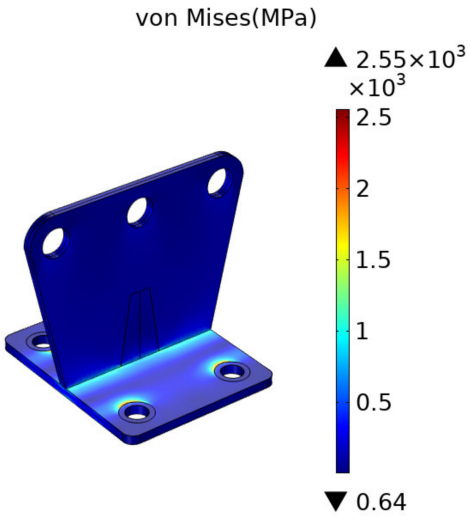

Figure 4. Von-Mises stress distribution of the original bracket.

From the result of the numerical simulation, the maximum von-Mises stress value of the original bracket structure is 2550 MPa and the von-Mises stress value at the connection between the vertical and horizontal plates is about 900 MPa. According to the material properties of TC4, the tensile strength of TC4 is 1075 MPa and the yield strength is 965 MPa, which can be found in the Electro Optical Systems (EOS) company official website. The stress of the original bracket during the loading process is close to the yield limit of the material and the structure may fail due to fatigue during the loading process of the fixture. For the purpose of reasonable stress distribution in the bracket and removal of excess material, this article utilizes topology optimization to redistribute the material in the design domain to achieve this goal.

3. Topology Optimization Model Considering Fatigue Characteristics

3.1. Multiple Load Case Model Considering Fatigue Characteristics

In this article, the required material for the design is TC4, which has a higher yield limit compared with steel and aluminum alloy. When the bolts are tightened, the upper fixture loading of the bracket is loaded symmetrically with the four screw holes fixed at the bottom. In this situation, the stress state is relatively balanced. Therefore it is considered that the bracket has a low probability of fatigue failure during the normal loading of the fixture. As the bracket is loaded for a considerable time, the bolts using for fixing the bracket are probably loosened under the cyclic load, at which time the loading condition of the fixture will appear asymmetrically loaded in a localized way. Due to the asymmetric loading, the bracket will be deformed asymmetrically, which will eventually lead to excessive stress. Accordingly, it is assumed that the probability of fatigue under these asymmetric conditions with fixture loading is much greater than the probability of fatigue under normal loading. Therefore, this paper proposes to transform the fatigue damage problem of the bracket in the cyclic loading process into the topology optimization problem that controls the strain energy of the bracket under a variety of extreme conditions and to combine the geometric reconstruction to smooth the region with large stress values, so as to reduce the overstress phenomena caused by geometric singularities. By controlling the strain energy and stress magnitude under extreme operating conditions, the probability of fatigue failure of the bracket can be reduced even if it is subjected to cyclic loading for a long time and the service life of the bracket can be extended.

In this paragraph, the external loads and boundary conditions for our proposed extreme operating conditions are presented in detail. First, the original bracket bolt hole designations are agreed as shown in Figure 5; the three bolt holes in the upper part of the vertical plate are assigned the designations A, B, and C; the four bolt holes in the lower bottom plate are assigned the designations a, b, c, and d in clockwise order. A total of 19 extreme working conditions in which the bolt may fail have been summarized with the fixture loaded and the specific parameters are shown in Table 2. Among these conditions, from 1 to 15 conditions are asymmetric loaded and the last four conditions are symmetric loaded. It is assumed that each condition is subject to six varieties of identical loads. When the vertical plate bolt hole is loosened, it is assumed that the screw will be in contact with the upper half of the bolt hole, the lower half of the bolt hole, the left half of the bolt hole, or the right half of the bolt hole respectively and the magnitude of these loads are 0.2 times the magnitude of the loads in the vertical direction. The six kinds of loads in the first condition are shown in Figure 6 and the other conditions can easily be constructed referring to condition 1.

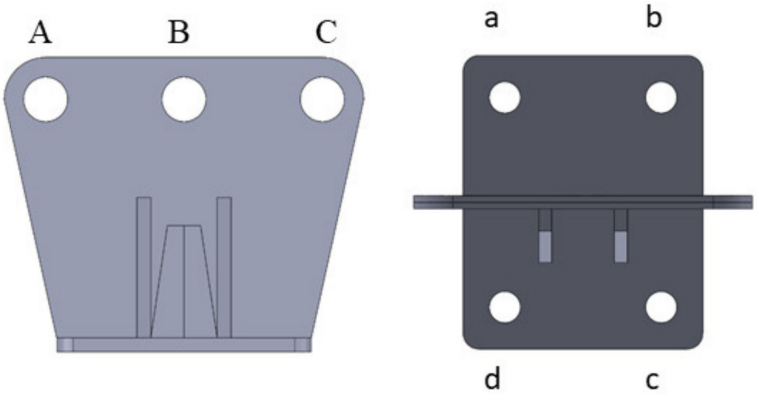

Figure 5. The designations of the bolt holes. A, B, C represent the locations of bolt holes in vertical plate; a, b, c, d represent the location of bolt holes in low bottom plate.

Table 2. Extreme conditions list. A,B represent bolt holes A and B are loaded while bolt hole C is unloaded; A,C represent bolt holes A and C are loaded while bolt hole B is unloaded; B,C represent bolt holes B and C are loaded while bolt hole A is unloaded; A,B,C represent bolt A, B, and C are all loaded; a,b,c,d represent bolt hole a, b, c, and d are all fixed; a,b,c represent bolt holes a, b, and c are fixed while bolt hole d is unconstrained; a,b,d represent bolt holes a, b, and d are fixed while bolt hole c is unconstrained; a,c,d represent bolt holes a, c, and d are fixed while bolt hole b is unconstrained; b,c,d represent bolt holes b, c, and d are fixed while bolt hole a is unconstrained.

Extreme Condition Sequence	External Loads Location	Fixed Boundary Location	The Number of Multiple Load Cases
1	A,B	a,b,c,d	6
2	A,C	a,b,c,d	6
3	B,C	a,b,c,d	6
4	A,B	a,b,c	6
5	A,B	a,b,d	6
6	A,B	a,c,d	6
7	A,B	b,c,d	6
8	A,C	a,b,c	6
9	A,C	a,b,d	6
10	A,C	a,c,d	6
11	A,C	b,c,d	6
12	B,C	a,b,c	6
13	B,C	a,b,d	6
14	B,C	a,c,d	6
15	B,C	b,c,d	6
16	A,B,C	a,b,c	6
17	A,B,C	a,b,d	6
18	A,B,C	a,c,d	6
19	A,B,C	b,c,d	6

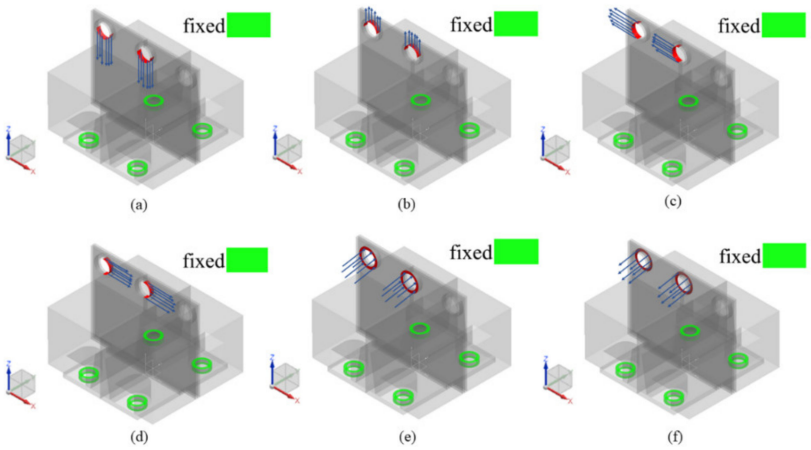

Figure 6. Six kinds of loads in condition 1. The green regions are fixed boundary conditions. The red regions are the location of external loads. (**a**) represents the first load case in condition 1; (**b**) represents the second load case in condition 1; (**c**) represents the third load case in condition 1; (**d**) represents the fourth load case in condition 1; (**e**) represents the fifth load case in condition 1; (**f**) represents the sixth load case in condition 1.

3.2. Topology Optimization Model Formulation

In this paper, the bracket is subjected to cyclic loading in the vertical direction during fixture loading. To satisfy fatigue resistance, it is suggested to convert this fatigue resistance problem into a problem of minimizing the mean compliance of the structure under the 19 extreme operating conditions. Ignoring damping effect, the mathematical formulation of the topology optimization model is as follows:

$$\begin{aligned} \min f(\boldsymbol{\rho}) : & \sum_{i=1}^{n} \alpha_i \left(\mathbf{F}_i^T \mathbf{U}_i(\omega;\rho)\right)^2 \\ s.t. : & \left(\mathbf{K}_1(\boldsymbol{\rho}) - \omega^2 \mathbf{M}_1(\boldsymbol{\rho})\right)\mathbf{U}_i = \mathbf{F}_i, i = 1,2,3 \\ & \left(\mathbf{K}_2(\boldsymbol{\rho}) - \omega^2 \mathbf{M}_2(\boldsymbol{\rho})\right)\mathbf{U}_i = \mathbf{F}_i, i = 4,8,12,16 \\ & \left(\mathbf{K}_3(\boldsymbol{\rho}) - \omega^2 \mathbf{M}_3(\boldsymbol{\rho})\right)\mathbf{U}_i = \mathbf{F}_i, i = 5,9,13,17 \\ & \left(\mathbf{K}_4(\boldsymbol{\rho}) - \omega^2 \mathbf{M}_4(\boldsymbol{\rho})\right)\mathbf{U}_i = \mathbf{F}_i, i = 6,10,14,18 \\ & \left(\mathbf{K}_5(\boldsymbol{\rho}) - \omega^2 \mathbf{M}_5(\boldsymbol{\rho})\right)\mathbf{U}_i = \mathbf{F}_i, i = 7,11,15,19 \\ & \sum \rho_{nd} v_{nd} <= V_0 \\ & 0 < \delta < \rho_{nd} < 1, nd = 1,2,\ldots,l \end{aligned} \tag{1}$$

where f is the objective value function, $\omega(\omega = 20\pi, \mathrm{rad/s})$ is the prescribed angular frequency, i is the number of the extreme conditions, n is the maximum number of extreme condition, nd is the number of nodes which are discretized by FEM, l is the maximum number of nodes,α_i is the weighted coefficient, $\mathbf{K}(\boldsymbol{\rho})$ is the global stiffness matrix penalized by the SIMP method and $\mathbf{K}_1, \mathbf{K}_2, \ldots, \mathbf{K}_5$ mean that there are five kinds of boundary conditions in FEM, $\mathbf{M}(\boldsymbol{\rho})$ is the global mass matrix penalized by the SIMP method and $\mathbf{M}_1, \mathbf{M}_2, \ldots, \mathbf{M}_5$ mean that there are five kinds of boundary conditions in FEM, $\mathbf{U}_i$ is a vector of node displacements, $\mathbf{F}_i$ is the loading vector, V_0 is the allowed fraction of total material volume, $\delta(\delta = 0.001)$ is the lower boundary of the design variable to prevent singularities in the global matrix. Considering that there are six load cases in each extreme condition, it means:

$$\mathbf{U}_i = [\mathbf{U}_i^1\ \mathbf{U}_i^2\ \mathbf{U}_i^3\ \mathbf{U}_i^4\ \mathbf{U}_i^5\ \mathbf{U}_i^6] \tag{2}$$

$$\mathbf{F}_i = [\mathbf{F}_i^1\ \mathbf{F}_i^2\ \mathbf{F}_i^3\ \mathbf{F}_i^4\ \mathbf{F}_i^5\ \mathbf{F}_i^6] \tag{3}$$

where superscript 1, 2, . . . , 6 are indexes which represent load cases in each extreme condition. For each load case, for example

$$(\mathbf{K}_1(\boldsymbol{\rho}) - \omega^2\mathbf{M}_1(\boldsymbol{\rho}))\mathbf{U}_1^1 = \mathbf{F}_1^1 \tag{4}$$

where $\mathbf{K}_1(\boldsymbol{\rho}) - \omega^2\mathbf{M}_1(\boldsymbol{\rho})$ needs to be decomposed as $\mathbf{K}_1(\boldsymbol{\rho}) - \omega^2\mathbf{M}_1(\boldsymbol{\rho}) = \mathbf{LU}$ via LU decomposition. $\mathbf{L}$ is the lower triangular matrix and $\mathbf{U}$ is the upper triangular matrix. Because matrix $\mathbf{K}_1$ and $\mathbf{M}_1$ is unchanged for different load cases, if the boundary conditions are the same in FEM, the LU decomposition is only implemented once for every boundary condition and matrix $\mathbf{L}$ and $\mathbf{U}$ are saved in the memory. Substituting matrix $\mathbf{L}$ and $\mathbf{U}$ in Equation (4) to solve this is much faster than directly solving it. Other load cases have the same procedure.

3.3. Sensitivity Analysis

Consider that the objective function in this optimization is the mean compliance and the load on the bracket is the mechanical force with prescribed angular frequency. According to article [19], the sensitivity of the objective function $f(\boldsymbol{\rho})$ with respect to the design variables $\boldsymbol{\rho}$, while the weighted coefficients and the sequence number of boundary conditions are neglected, is given by

$$\frac{\partial f}{\partial \boldsymbol{\rho}} = 2\mathbf{F}_i^T\mathbf{U}_i\left(\frac{\partial \mathbf{F}_i^T}{\partial \boldsymbol{\rho}}\mathbf{U}_i + \mathbf{F}_i^T\frac{\partial \mathbf{U}_i}{\partial \boldsymbol{\rho}}\right) \tag{5}$$

The sensitivity of F_i^T with respect to design variables $\boldsymbol{\rho}$ will be zero if the load is design-independent. In this article, the mechanical force is design-independent. The sensitivity of displacement vector $\mathbf{U}$ with respect to design variables $\boldsymbol{\rho}$ is given by

$$(\mathbf{K}(\boldsymbol{\rho}) - \omega^2\mathbf{M}(\boldsymbol{\rho}))\frac{\partial \mathbf{U}_i}{\partial \boldsymbol{\rho}} + \left(\frac{\partial \mathbf{K}(\boldsymbol{\rho})}{\partial \boldsymbol{\rho}} - \omega^2\frac{\partial \mathbf{M}(\boldsymbol{\rho})}{\partial \boldsymbol{\rho}}\right)\mathbf{U}_i = \frac{\partial \mathbf{F}_i}{\partial \boldsymbol{\rho}} \tag{6}$$

Instead of solving Equation (6), the adjoint method (see [20]) may be used to calculate the sensitivity of the objective function in a more efficient manner, which gives the following result

$$\frac{\partial f}{\partial \boldsymbol{\rho}} = -2\mathbf{F}_i^T\mathbf{U}_i\left[\mathbf{U}_i{}^T\left(\frac{\partial \mathbf{K}(\boldsymbol{\rho})}{\partial \boldsymbol{\rho}} + \omega^2\frac{\partial \mathbf{M}(\boldsymbol{\rho})}{\partial \boldsymbol{\rho}}\right)\mathbf{U}_i\right] \tag{7}$$

where the sensitivities of the stiffness and mass matrices can be directly obtained from the SIMP material model

$$\frac{\partial \mathbf{M}(\boldsymbol{\rho})}{\partial \boldsymbol{\rho}} = \sum_{nd}^{l}\mathbf{M}_0 \tag{8}$$

$$\frac{\partial \mathbf{K}(\boldsymbol{\rho})}{\partial \boldsymbol{\rho}} = \sum_{nd}^{l}p\rho_{nd}^{p-1}\mathbf{K}_0 \tag{9}$$

where $\mathbf{K}_0$ is the element stiffness matrix, $\mathbf{M}_0$ is the element mass matrix.

In order to avoid topology optimization results falling into local minima, checkerboard, and numerical instabilities, a sensitivity filter or density filter techniques are often introduced into the calculation of topology optimization [21]. In this paper sensitivity filtering is used to achieve clear boundaries of the topology optimization result. To generate the weighted matrix of the filter, the matrix form of the discrete Laplace equation under the finite element method with the nodes as design variables is applied. In COMSOL, this method is characterized by high efficiency, easy implementation, good filtering performance, and little external filter parameters.

3.4. Solving Strategy

In this paper, there are 114 load cases in the process of solving the finite element equilibrium equations under various operating conditions. In COMSOL software, we

can utilize parametric sweeping for efficient solving. Neglecting the boundary condition sequence numbers, the mathematical formulation can be written as follows

$$\mathbf{K}[\mathbf{U}_1\ \mathbf{U}_2\ \ldots\ \mathbf{U}_{n'}] = [\mathbf{F}_1\ \mathbf{F}_2\ \ldots\ \mathbf{F}_{n'}] \tag{10}$$

where every kind of load case will be assembled in the right hand side of the equilibrium equation with FEM. The global stiffness matrix is inversed by means of LU decomposition so that the inverse matrix is solved only once in the multi-load problem. If the solution is not solved by parametric sweeping, the multi-load cases will get the following mathematical expression

$$\begin{array}{c} \mathbf{K}\mathbf{U}_1 = [\mathbf{F}_1] \\ \mathbf{K}\mathbf{U}_2 = [\mathbf{F}_2] \\ \vdots \\ \mathbf{K}\mathbf{U}_{n'} = [\mathbf{F}_{n'}] \end{array} \tag{11}$$

This means that the number of inverse matrixes solved is equal to the number of multi-load cases. In this article, the total number of load cases is 114. If parameter sweeping is not utilized, it is necessary to solve the inverse matrix 114 times. However, it only needs to be solved five times in parameter sweeping considering the five different constraints in FEM. Therefore, the efficiency of solving is greatly improved.

4. Numerical Result and Geometric Reconstruction

4.1. Numerical Result

Before topology optimization, it is necessary to expand the design space referring to the original bracket. Meanwhile, it is necessary to remove part of the design space on both sides of the connected fixture because the three bolt holes above the vertical plate need to be connected to the fixture. Four bolt holes at the bottom of the horizontal plate also need to be connected to the fixture, but it is required to leave part of the assembly space above the bolt holes. To ensure some necessary geometric features, there are some non-design domains in the design space, the final geometry is shown in Figure 7. In FEM, the geometry is discretized in mesh with linear tetrahedron elements. There are 263,297 tetrahedron elements in this mesh and the number of vertices of the mesh is 367,249. The picture of the mesh is shown in Figure 8. The objective function of topology optimization is the minimum compliance problem under multiple conditions with the number of conditions n = 19. In each condition, it is a multi-load problem with six load cases. In this article, the initial value of design variables $\boldsymbol{\rho}$ are all 0.5, the penalty factor is p = 4, Young's modulus $E = 1.1 \times 10^{11}$ Pa, Poisson's ratio $\nu = 0.34$, the density of material is 4.51×10^3 kg/m^3. The design variables are updated with the universal and robust MMA [22] algorithm and the final post-processing results of the topology optimization are shown in Figure 9.

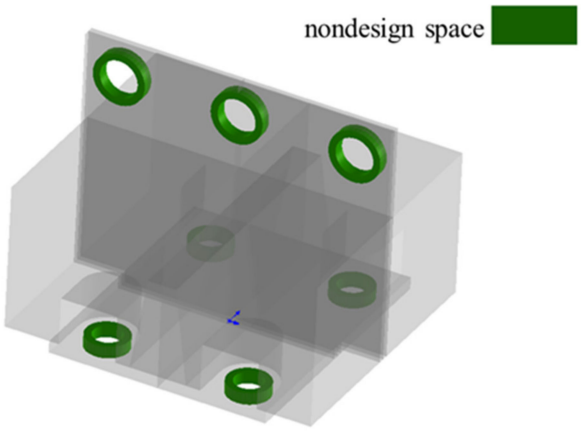

Figure 7. Schematic diagram of non-design space.

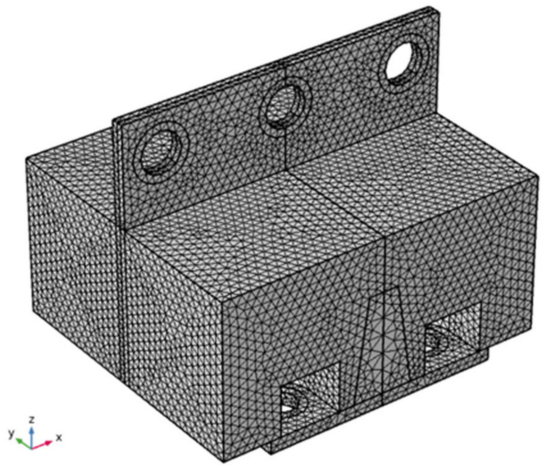

Figure 8. Discrete mesh diagram.

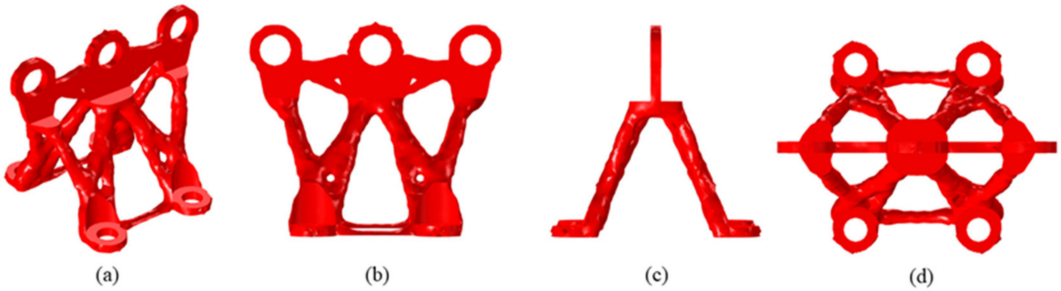

Figure 9. (**a**) Represents the isometric view of the result; (**b**) represents the front view of the result; (**c**) represents the side view of result; (**d**) represents the top view of the result.

4.2. Geometry Reconstruction

Although the existing commercial software can automatically fit the topology optimization results with surfaces to generate solid geometry files, the fitting accuracy cannot satisfy the assembly requirements of the fatigue tester fixture. So the post-processing result is required to be reconstructed by CAD software and the reconstructed geometry is shown in Figure 10. In the process of geometric reconstruction, bars are added to some regions to improve the stability of the structure, based on engineering experience, and also to lighten several places where the stresses are concentrated, from which some inessential regions are deleted, thus reducing the mass of the structure. A comparison of the reconstructed geometry and topology optimization result is shown in Figure 11. The numerical simulation results of the reconstructed geometry with the same boundary conditions and external load are shown in Figure 12. The mesh is shown in Figure 13 and quadratic elements are applied in the FEM analysis. The number of elements are 249,195 and the number of nodes are 403,126. The stress singularity is neglected in fixed boundary condition regions. The main region's von-Mises stress is about 470 MPa. The mass of the reconstructed geometry is 285.7 g and the weight is reduced about 37% compared to the original 480 g. The application of topology optimization technology significantly changed the force transmission path of the structure, reducing the weight of the structure while making the stress distribution more reasonable, thus improving the mechanical properties of the structure. However, it is also because of the use of topology optimization that the new aerospace bracket is difficult to manufacture by traditional mechanical processing methods whereas the use of 3D-printing makes it relatively easy to manufacture parts of such a complex configuration, such as the new bracket. The new bracket is fabricated by EOS M290, which allows a fast, flexible, and cost-effective production of metal parts directly from CAD data. EOS Titanium Ti64 is used as metal powder in 3D-printing and more information about which

is presented in the EOS official website. The final structure generated by metal 3D-printing is shown in Figure 14.

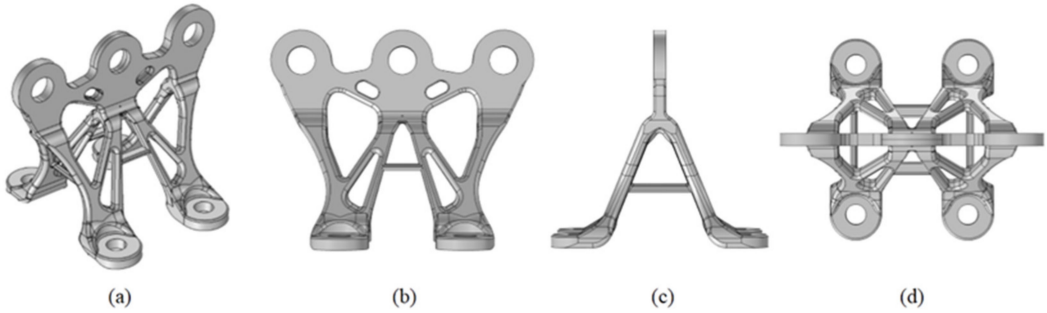

Figure 10. (**a**) Isometric view after reconstruction; (**b**) front view after reconstruction; (**c**) side view after reconstruction; (**d**) top view after reconstruction.

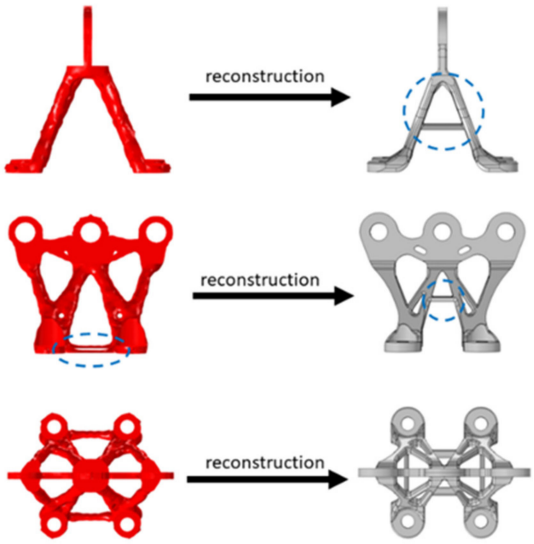

Figure 11. Comparison of topology optimization result and reconstructed geometry.

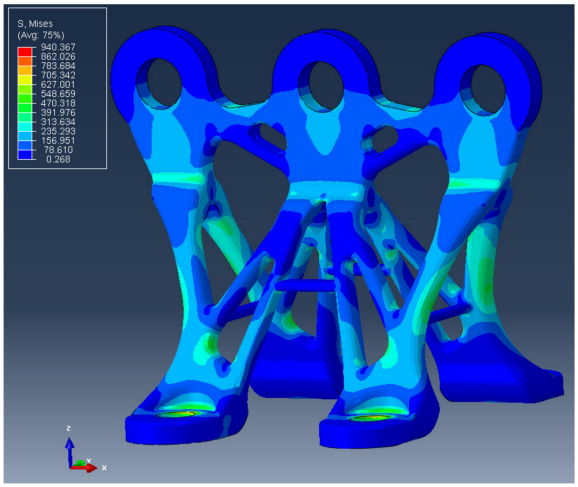

Figure 12. The numerical simulation result of the reconstructed geometry subjected to 50 kN vertical load.

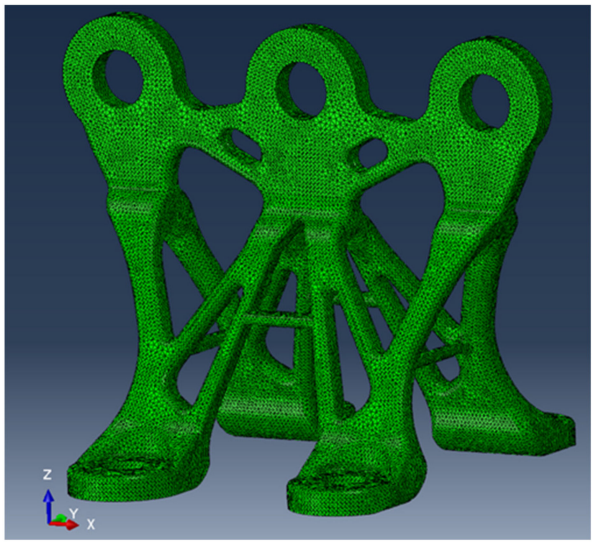

Figure 13. The mesh diagram of new bracket.

Figure 14. New bracket after 3D-printing with EOS M290.

5. Fatigue Test Procedure and Result

The fatigue test was commissioned by our co-operator (AECC Beijing Institute of Aeronautical Materials, Beijing, China) and carried out by AVIC Touchstone Testing Innovation (DaChang) Company (Langfang City, Hebei Province, China). The fatigue tester type used in this fatigue test is MTS-250kN-1 and the test temperature is room temperature. The machine loading control method is stress control and the loading waveform is sine wave of frequency 10 Hz. Due to the limitation of the test conditions, the demand condition of the initial fatigue test of the designed bracket was not used in this fatigue test, in which the maximum magnitude was 50 kN and the minimum magnitude was 5 kN sine load in the vertical direction. The used maximum magnitude was 100 kN and the minimum magnitude was 10 kN sine load in the vertical direction instead. The upper and lower parts of the 3D printed bracket without heat treatment were connected to the fatigue tester by bolts as shown in Figure 15. As the fatigue test was conducted, the number of cycles in which the 3D-printing bracket fracture was 6201. The picture of the bracket fractured during the test is shown in Figure 16. The fatigue life of the parts in engineering are usually presented as S-N curve characteristics and the S-N curve is a negative exponential curve. In paper [23], it is stated that the fatigue properties of parts obtained with 3D-printing are

similar to the parts obtained with traditional manufacturing processes. According to [24], the formulation of the fitted S-N curve of TC4 is given by

$$\sigma(N) = [1700(N - 4900)^{-0.2} + 440]\text{MPa} \quad (12)$$

where $\sigma(N)$ is the stress amplitude and in this paper von-Mises was used, N is the number of test cycles. First, it is necessary to verify that Equation (12) is suitable for the new bracket. As shown in Figure 17, the von-Mises stress of main region in new bracket subjected to 100 kN vertical load is about 940 MPa. $\sigma(N)$ is substituted with 940 MPa in Equation (12) and the number of the test cycles obtained is about 5354. Compared with the practiced fatigue test, the error of calculation is 13.7%, which is within the acceptable range in engineering. When the maximum von-Mises 470 MPa is substituted in Equation (12), it can be inferred that when the new bracket is subjected to a maximum load of 50 kN and a minimum load of 5 kN sine load in the vertical direction, the number of cycles is about 5.84×10^8, exceeding the engineering specifications proposed at the beginning of the bracket design. As the new bracket is manufactured by laser selective melting (SLM), the characteristics of SLM are a good surface finish and a high residual stress, where a good surface finish can improve the fatigue life of the part, while a higher residual stress can have a serious negative impact on the fatigue performance of the material. According to the literature [25], the most desirable heat treatment in the 3D printing manufacturing process is hot isostatic pressing, which can not only relieve residual stresses but also eliminate the hole defects prevalent in 3D printed titanium alloys. Consequently, there is potential for further improvement in the fatigue performance of 3D printed aerospace brackets.

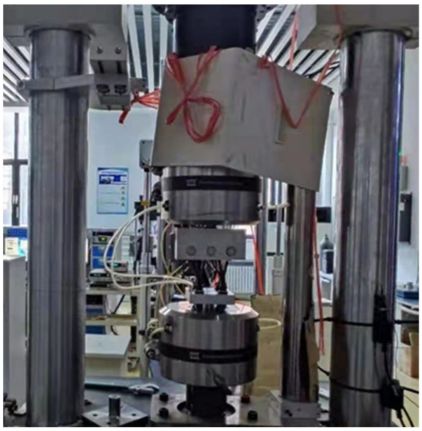

Figure 15. New bracket with the actual fatigue tester machine assembly diagram.

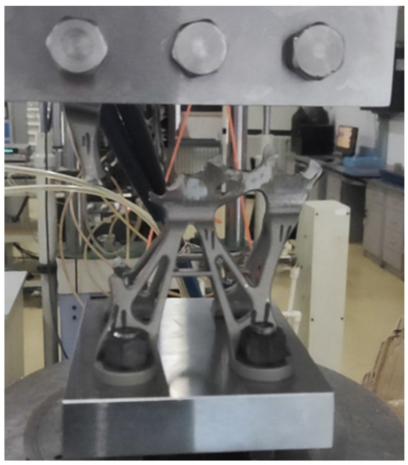

Figure 16. New bracket fracture during the fatigue test by MTS-250kN-1.

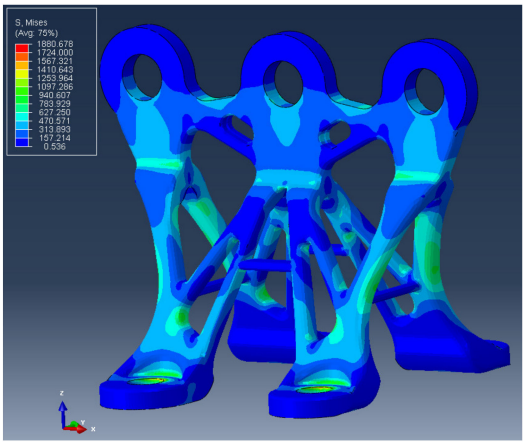

Figure 17. The numerical simulation result of reconstructed geometry subjected to 100 kN vertical load.

6. Conclusions

The 3D-printing technology provides a broad possibility for manufacturing. The topology optimization technology provides an important way to design high-performance lightweight structures. This paper proposed a combination of topology optimization and 3D-printing technology for designing and manufacturing of an aerospace bracket considering the fatigue performance. In this approach, the fatigue damage problem of the bracket in cyclic loading was transformed into a topology optimization problem that controls the bracket with minimal strain energy under a variety of extreme operating conditions, based on the real operating environment of the bracket. Under the guidance of the topology optimization result considering fatigue performance, a new aerospace bracket was redesigned by CAD software, and fabricated by SLM. The mass of the fabricated new bracket was reduced by 37% compared with the original bracket structure. Both the numerical simulation and fatigue test were implemented to verify the reliability of the new bracket structure. The numerical simulation shows that the new bracket has a reasonable stress distribution compared with the original bracket. The fatigue test perfectly fulfills the engineering specifications proposed at the beginning of the bracket design. Both approaches validate the effectiveness of our proposed new design method. This work indicates that the integration of the proposed topology optimization design method and additive manufacturing can be a powerful tool for the design of lightweight structures considering the fatigue performance.

Author Contributions: Conceptualization, Q.W. and C.W. and Z.L.; methodology, Q.W. and Z.L; software, Z.L.; validation, Y.C. and C.W.; investigation, Y.S. and P.G.; resources, Y.Y. and Z.L.; writing—original draft preparation, Y.C.; writing—review and editing, Y.C. and Z.L.; formal analysis, Y.C. and C.W.; visualization, Y.S. and P.G; supervision, Q.W. and Z.L. All authors have read and agreed to the published version of the manuscript.

Funding: This research was funded by the National Science Foundation of China (grant Nos.51675506); the Foundation for Excellent Young Scholars of Jilin Province, China (grant number 20190103015JH).

Institutional Review Board Statement: Not applicable.

Informed Consent Statement: Not applicable.

Data Availability Statement: If readers want to obtain original data in the paper, please contact with correspondence Z.L.

Acknowledgments: The fatigue test in this work was implemented by the AECC Beijing Institute of Aeronautical Materials (Beijing, China) and AVIC Touchstone Testing Innovation (DaChang) Company (Langfang City, Hebei Province, China).

Conflicts of Interest: The authors declare no conflict of interest.

References

1. Gu, D.D.; Meiners, W.; Wissenbach, K.; Poprawe, R. Laser Additive Manufacturing of Metallic Components: Materials, Processes and Mechanisms. *Int. Mater. Rev.* **2013**, *57*, 133–164. [CrossRef]
2. Bendsøe, M.P.; Sigmund, O. *Topology Optimization—Theory, Methods, and Applications*; Springer Verlag: Berlin/Heidelberg, Germany, 2003; ISBN 978-3-642-07698-5.
3. Shi, G.; Guan, C.; Quan, D.; Wu, D.; Tang, L.; Gao, T. An Aerospace Bracket Designed by Thermo-Elastic Topology Optimization and Manufactured by Additive Manufacturing. *Chin. J. Aeronaut.* **2020**, *33*, 1252–1259. [CrossRef]
4. Jihong, Z.; Fei, H.; Weihong, Z. Key Optimization Design Issues for Achieving Additively Manufactured Aircraft and Aerospace Structures. *Aeronaut. Manuf. Technol.* **2017**, *5*, 16–21. [CrossRef]
5. Dbouk, T. A Review about the Engineering Design of Optimal Heat Transfer Systems Using Topology Optimization. *Appl. Therm. Eng.* **2017**, *112*, 841–854. [CrossRef]
6. Beghini, L.L.; Beghini, A.; Katz, N.; Baker, W.F.; Paulino, G.H. Connecting Architecture and Engineering through Structural Topology Optimization. *Eng. Struct.* **2014**, *59*, 716–726. [CrossRef]
7. Tomlin, M.; Meyer, J. Topology Optimization of an Additive Layer Manufactured (Alm) Aerospace Part. In Proceedings of the 7th Altair CAE Technology Conference, Warwickshire, UK, 10 May 2011.
8. Liang, M.; Weihong, Z.; Dongliang, Q.; Guanghui, S.; Lei, T.; Yuliang, H.; Piotr, B.; Jihong, Z.; Tong, G. From Topology Optimization Design to Additive Manufacturing: Today's Success and Tomorrow's Roadmap. *Arch. Comput. Methods Eng.* **2020**, *27*, 805–830. [CrossRef]
9. Jihong, Z.; Han, Z.; Chuang, W.; Lu, Z.; Shangqin, Y.; Weihong, Z. Status and Future of Topology Optimization for Additive Manufacturing. *Aeronaut. Manuf. Technol.* **2020**, *63*, 24–38. [CrossRef]
10. Eschenauer, H.A.; Olhoff, N. Topology Optimization of Continuum Structures: A Review. *Appl. Mech. Rev.* **2001**, *54*, 331–390. [CrossRef]
11. Sigmund, O.; Maute, K. Topology Optimization Approaches. *Struct. Multidiscip. Optim.* **2013**, *48*, 1031–1055. [CrossRef]
12. Rozvany, G.I. A Critical Review of Established Methods of Structural Topology Optimization. *Struct. Multidiscip. Optim.* **2009**, *37*, 217–237. [CrossRef]
13. Jie, H.; Jihong, Z.; Chuang, W.; Jie, W.; Weihong, Z. Topology Optimization of the Multi-Fasteners Jointed Structure Considering Joint Load Constraint and Fatigue Constraints. *Chin. Sci. Bull.* **2018**, *64*, 79–86. [CrossRef]
14. Shanglong, Z.; Chau, L.; Arun, L.G.; Julián, A.N. Fatigue-Based Topology Optimization with Non-Proportional Loads. *Comput. Methods Appl. Mech. Eng.* **2019**, *345*, 805–825. [CrossRef]
15. Desmorat, B.; Desmorat, R. Topology Optimization in Damage Governed Low Cycle Fatigue. *Comptes Rendus Mec.* **2008**, *336*, 448–453. [CrossRef]
16. Collet, M.; Bruggi, M.; Duysinx, P. Topology Optimization for Minimum Weight with Compliance and Simplified Nominal Stress Constraints for Fatigue Resistance. *Struct. Multidiscip. Optim.* **2017**, *55*, 839–855. [CrossRef]
17. Holmberg, E.; Torstenfelt, B.; Klarbring, A. Fatigue Constrained Topology Optimization. *Struct. Multidiscip. Optim.* **2014**, *50*, 207–219. [CrossRef]
18. Nabaki, K.; Shen, J.; Huang, X. Evolutionary Topology Optimization of Continuum Structures Considering Fatigue Failure. *Mater. Des.* **2019**, *166*, 107586. [CrossRef]
19. Olhoff, N.; Du, J. Topological Design for Minimum Dynamic Compliance of Structures under Forced Vibration. *Topol. Optim. Struct. Contin. Mech.* **2014**, 325–339. [CrossRef]
20. Tortorelli, D.A.; Michaleris, P. Design Sensitivity Analysis: Overview and Review. *Inverse Problems Eng.* **1994**, *1*, 71–105. [CrossRef]
21. Sigmund, O.; Maute, K. Sensitivity Filtering from a Continuum Mechanics Perspective. *Struct. Multidiscip. Optim.* **2012**, *46*, 471–475. [CrossRef]
22. Svanberg, K. The Method of Moving Asymptotes—A New Method for Structural Optimization. *Int. J. Numer. Methods Eng.* **1987**, *24*, 359–373. [CrossRef]
23. Beretta, S.; Romano, S. A Comparison of Fatigue Strength Sensitivity to Defects for Materials Manufactured by Am or Traditional Processes. *Int. J. Fatigue* **2017**, *94*, 178–191. [CrossRef]
24. Janeček, M.; Nový, F.; Harcuba, P.; Stráský, J.; Trško, L.; Mhaede, M.; Wagner, L. The Very High Cycle Fatigue Behaviour of Ti-6Al-4V Alloy. *Acta Phys. Pol. A.* **2015**, *128*, 497–503. [CrossRef]
25. Edwards, P.; Ramulu, M. Fatigue Performance Evaluation of Selective Laser Melted Ti–6Al–4V. *Mater. Sci. Eng. A* **2014**, *598*, 327–337. [CrossRef]